Blind SELEX Approach Identifies RNA aptamer that Regulate EMT and Inhibit Metastasis

Sorah Yoon[1], Brian Armstrong[2], Nagy Habib[3] and John J Rossi[1,4,*]

1. Department of Molecular and Cellular Biology, Beckman Research Institute of City of Hope, Duarte, California, USA
2. Light Microscopy core, City of Hope, Duarte, California, USA
3. Department of Surgery and Cancer, Imperial College London, London, UK
4. Irell and Manella Graduate School of Biological Sciences, Beckman Research Institute of City of Hope, Duarte, California, USA

Running title: Anti-vimentin RNA Aptamer in Pancreatic Cancer

Keywords: RNA aptamer, Vimentin, Tumor cell metastasis

Financial support: the National Institutes of Health R01 AI029329 to J.J.R. and Apterna Ltd.

Disclosure of Potential Conflict of Interest: S.Y., N.H., and J.J.R. hold stocks in Apterna Ltd. U.K.

* Correspondence should be addressed to: J.J.R. (jrossi@coh.org), Beckman Research Institute of City of Hope, 1500 East Duarte Rd, Duarte, CA 91010, USA, fax: 626-301-8271, phone: 626-301-8390

Abstract

Identifying targets that are exposed on the plasma membrane of tumor cells, but expressed internally in normal cells, is a fundamental issue for improving the specificity and efficacy of anticancer therpeutics. Using blind cell SELEX (Systemic Evolution of Ligands by EXponetial enrichment) which is untargeted SELEX, we have identified an aptamer, P15, which specifically bound to the human pancreatic adenocarcinoma cells. To identify the aptamer binding plasma membrane protein, liquid chromatography tandem mass spectrometry (LC-MS/MS) was used. The results of this unbiased proteomic mass spectrometry approach identified the target of P15 as the intermediate filament vimentin, biomarker of epithelial mesenchymal transition (EMT), which is an intracellular protein but is specifically expressed on the plasma membrane of cancer cells. As EMT plays a pivotal role to transit cancer cells to invasive cells, tumor cell metastasis assays were performed *in vitro*. P15 treated pancreatic cancer cells showed the significant inhibition of tumor metastasis. To investigate the downstream effects of P15, EMT related gene expression analysis was performed to identify differently expressed genes (DEGs). Among five DEGs, P15 treated cells showed the down-regulated expression of matrix metallopeptidase 3 (MMP3), which is involved in cancer invasion. These results, for the first time, demonstrate that P15 binding to cell surface vimentin inhibits the tumor cell invasion and is associated with reduced MMP3 expression. Thus, suggesting that P15 has potential as an anti-metastatic therapy in pancreatic cancer.

Implications: This study reveals that anti-vimentin RNA aptamers selected via blind-SELEX inhibits the tumor cell metastasis.

Introduction

Aptamers, which are small single-stranded and structured nucleic acids, are powerful and emerging molecular tools for identifying biomarkers in cancer, as they can be selected to recognize a variety of targets including proteins, cultured cells, and whole organisms (1-6). Aptamers are generated by **S**ystematic **E**volution of **L**igands by **EX**ponential enrichment (**SELEX**) and hold their three-dimensional structures using well-defined complementary nucleic acid sequences (7,8). Because aptamers adopt complex structures, they can bind targets with high affinity and specificity and offer significant advantages over antibodies; better structural stability, low toxicity, low immunogenicity, and greater safety (7,8).

Potential aptamer targets that are selectively expressed on the plasma membrane of cancer cells can be used to further understanding of tumor development and to develop improved targeted therapeutics. Ever since Berezovski *et al.* initiated aptamer-facilitated biomarker discovery (AptaBiD) (9), the identification and validation of biomarkers for therapeutics and the diagnosis of cancer has rapidly progressed; example biomarkers include: heat-shock protein 70 (HSP70) (10,11), heat-shock protein 90 (HSP90) (12,13), glucose-regulated protein 78 (GRP78) (14,15), vimentin (16), nucleolin (17,18), feto-acinar pancreatic protein (FAPP) (19), alkaline phosphatase placental-like 2 (ALPPL-2) (20), siglec-5 (21), stress-induced phosphoprotein 1 (STIP1) (22), and protein tyrosine kinase 7 (PTK7) (23). In pancreatic cancer, alkaline phosphatase placental-like 2 (ALPPL-2) and cyclophilin B have also been reported to be novel candidate biomarkers (20,24).

Pancreatic cancer is known to be one of the most deadly cancers and ranked as the fourth cause of cancer related death in both Europe and United States (25,26). Overall survival remains poor either in metastatic disease or in patients with early-stage disease (27). Mortality rate

remains high because most patients are diagnosed with metastatic stage of disease at first diagnosed. Pancreatic metastases can arise in any organ site, but are mostly detected in abdominal sites. In an autopsy series, the liver is found to be the most common site of metastasis, followed by the peritoneum and lung (28,29). Still, metastasis is the major cause of mortality in pancreatic cancer patients.

Over past years, great efforts have made to develop therapeutics to improve the mortality rate. However, there has been limited progress in therapeutic options for metastatic pancreatic cancer, and traditional chemotherapy outcomes, even though improved, are still disappointing. In this study, to select cancer specific biomarkers for increasing therapeutic intervention, blind cell-SELEX was employed against PANC-1 cells and liquid chromatography tandem mass spectrometry (LC-MS/MS) was used to identify the aptamer binding ligand.

Materials and Methods

Chemicals

Ultra-purified (Milli-Q) water, Acetonitrile (CH_3CN, Burdick and Jackson HPLC grade), Ammonium bicarbonate (NH_4HCO_3, Sigma), Dithiothreitol (DTT, Sigma), Iodoacetamide (IAA, Sigma), Trypsin (Promega modified trypsin, sequencing grade), Trifluroacetic acid (TFA, Sigma).

Blind SELEX (Naïve whole-Cell SELEX)

The following cell lines were purchased from the American Type Culture Collection (ATCC) for use as targets for SELEX and internalization assays: PANC-1 (CRL-1469), CFPAC-1 (CRL-1918), MIA PaCa-2 (CRL-1420), BxPC-3 (CRL-1687), and AsPC-1 (CRL-1682). Huh-

7 cells were purchased from Japanese Collection of Research Bioresources (JCRB). Cells were cultured according to the cell bank's instructions.

The SELEX cycle was performed basically as described by Tuerk and Gold (8) with few modifications which was carried out essentially as described (30).

Flow cytometry-based binding assays

Aptamer binding was also assessed by flow cytometry as described previously (30). To determine the apparent dissociation constant (K_D) of aptamers to PANC-1 cells, the mean fluorescence intensity (MFI) was calculated for each concentration and for the unselected library controls. The values for the controls were considered to be background fluorescence and were subtracted from the values for the aptamers, as previously described by Sefah et al. (31). The dissociation constants were calculated using a one-site binding model. Non-linear curve regression was performed using Graph Pad Prism (GraphPad Software, La Jolla, California, USA).

Live-cell confocal imaging

The aptamer internalization assay was determined described in previous studies (30). For the time-course internalization assay, 1×10^5 cells were seeded in 35 mm glass-bottom dishes (MatTek, MA, USA) and grown in medium for 24 hrs. Cy3 labeled P15 were added to the cells at 200 nM of final concentration and incubated for 30 minutes, 1 hours, 2 hours, 3 hours and 4 hours. Seven to eleven different locations of images were taken at each time points. Based on the Cy3 intensity on cells, the percentage was calculated.

Affinity purification of target membrane proteins and protein digestion

Biotinylated aptamers, together with associated protein complexes, were immobilized using a pull-down process. SELEX-selected RNA aptamers and control RNAs were labelled with biotin at their 3' ends. Target membrane proteins were isolated using procedures described by Daniels et al. (4). In-gel digestion was used for protein purification and analyzed by mass spectrometry for peptide fingerprinting. After polyacrylamide gel electrophoresis (SDS-PAGE), aptamer-retrieved protein bands were excised and in-gel digested (32).

Liquid chromatography Tandem MS/MS (LC-MS/MS) Q-TOF

An Agilent 6520 Q-TOF mass spectrometer equipped with a Chip Cube source was used for LC-MS/MS analyses. A C18 chip with a 43mm analytical column and a 40nl trapping column (ProtID-Chip-43, Agilent G4240-62005) was used. Digested samples (10-15 µl) were loaded onto the column at 6 µl/minute in 99% Buffer A (0.1% Formic Acid in water)/1% Buffer B (0.1% Formic Acid in Acetonitrile) with an extra 8 µl wash volume. The gradient was from 3% to 35% Buffer B over 8 minutes and then 35% to 90% Buffer B over 1 minute. The total run time, including injection, was 15 minutes. The voltage was adjusted to the 1850V to 2000V range. The X! Tandem search engine (http://www.thegpm.org/TANDEM/index.html) was used to search the peptide MS/MS spectrum. The dataset was then processed using the Scaffold program (http://www.proteomesoftware.com) to visualize the results. SWISS Prot or NCBI were used to obtain the detailed protein annotation.

Competition assays for validation of target

For the aptamer-antibody competition assay, Cy3-labeled P15 aptamer was used to

compete with vimentin antibodies (Sigma, V6630). The cells (1×10^5) were seeded in 35 mm glass-bottom dishes (MatTek, Ashland, MA, USA) and grown in medium for 24 hours. Cells were preincubated with vimentin antibodies, at 1 μM, for 20 minutes before Cy3-labeled P15, at 200 nM of final concentraion, was added. The cells were incubated for 2 hours at 37 °C. The images were taken using a Zeiss LSM 510 Meta Inverted 2-photon confocal microscope system using a C-Apo 40x/1.2NA water immersion objective. The arbitrary fluorescence intensity was quantified in the presence of vimentin antibodies competitors using confocal microscopy and analyzed statistically. Student's t test was used for statistical significance analysis ($P<0.05$).

For competition assay by flow cytometry, PANC-1 cells were detached using Accutase (Sigma-Aldrich), washed with DPBS, and suspended in binding. Next, PANC-1 cells were preincubated with vimentin antibodies, at 1 μM, for 20 minutes on ice. After preincubation with vimentin antibodies, Cy3-labeled aptamers at 200 nM of final concentration were added and incubated with 2×10^5 cells for 30 minutes on ice. Cells were washed with DPBS three times and immediately analyzed by Fortessa flow cytometry (BD Biosciences, San Jose, CA). 4'6'-diamidino-2-phenylindole (DAPI) (1μg/ml) was used to identify and exclude dead cells. Data were analyzed with FlowJo software (FlowJo, Ashland, OR).

Co-localization assay on live cells

The cells (1×10^5) were seeded in 35 mm glass-bottom dishes (MatTek, Ashland, MA, USA) and grown in medium for 24 hours. Cells were incubated with Cy3-labeled P15 at 500 nM of final concentration, vimentin antibodies at 1:1000 dilution with anti-mouse Alexa Fluor 488 antibodies at 1:2000 dilution for 1 hour at 37°C. After washing with DPBS three times, the images were taken using a Zeiss LSM 880 confocal laser scanning microscope with Airyscan

using a C-Apo 62x/1.2NA water immersion objective.

Biosensor assay

The Biacore T100 (GE Healthcare, Uppsala, Sweden) was used to monitor label-free the aptamer–vimentin interactions in real time. Biotinylated aptamers were coupled to a streptavidin-coated Biocore chip (SensorChip SA, BR-1003-98, General Electric Company) by an injection in binding buffer at concentration of 25 μg/mL at 10 μL/min. To measure binding kinetics, five concentration of vimentin protein were injected at a flow rate of 10 μL/min. After binding, the surface was regenerated by injecting 50 mM NaOH at flow rate of 15 μL per minutes for 20 seconds. Data from the control surface were subtracted. BIAevaluation software (GE Healthcare) was used for analysis. The binding data were fit to a 1:1 binding with a mass transfer model.

Tumor cell migration assay

Wound healing assays were performed with PANC-1 cells as described previously (33). Briefly, $1x10^6$ PANC-1 cells were seeded in 35mm dishes and grown into a monolayer culture with 100% confluency. After scratching through the monolayer with a pipette tip, media were replaced with DMEM. 3000 nM of final concentration of folded P15 was added into media after scratching. The images were taken at 12hrs, 18hrs and 24hrs. Image Pro Premier v9.2 (Media Cybernetics, Rockville, MD) was used to quantify the wound distance by first making a calibration from an image of a stage micrometer. The calibration was applied to the images in the wound healing assay so that the distance could be reported in microns. In Image Pro Premier the

wound distance was measured using the Line Tool in Measurements and the values were exported to Microsoft Excel for statistical analysis.

Tumor cell invasion assay

Tumor cell invasion assay was performed using the IncuCyte live-cell imaging system (ESSEN Bioscience) described previously (34). Cells were plated in IncuCyte ClearView 96-well cell migration plates for direct visualization of cell migration using phase-contrast. Cells were added to the top chamber of the ClearView plate and allowed to settle at ambient temperature with or without compounds. Images were taken for 2 days. 20% FBS was used as chemoattractant for positive control. Integrated metrics quantified the chemotactic response using 1,000 cells per well. Data was normalized with negative control. Each group is quadruplicate. Student's t test was used for statistical significance analysis.

Serum stability assay

P15 was folded in folding buffer and incubated at 37 ^{o}C with the same volume of 100 % human serum or 100 % mouse serum, which is at the final concentration of 50 %. At each time points of 0, 0.5, 1, 2, 3, 4, 5, 6, 24, 48 hours, 10 μL of P15 was mixed with denature gel loading dye. 10 % denature PAGE gel was used to run the samples. Quantification of the bands was performed using Biorad Image Lab software. The aptamer half-lives were calculated by fitting the curve to the non-linear one-phase decay model using Graph Pad Prism.

Gene expression analysis

1×10^5 cells were seeded in 6 well plates one day before the treatment. 1 μM of P15 was

incubated in cells for 48hrs. Total RNA was extracted and converted to cDNA by iScript reverse transcriptase (Bio-Rad, CA). Qiagen EMT RT^2 profiler PCR array was used to analysis EMT related gene expression.

Relative gene expression analysis by qPCR

For analyzing gene down regulation, PANC-1, Mia PaCa-2 and BxPC-3 cells were seeded into 24-well plates at a density of 1×10^5 cells per well. P15 or irrelevant aptamer were added directly to the cells, in triplicate, at a final concentration of 1 μM. Total RNA was extracted (RNeasy mini kit, Qiagen) and converted to cDNA (iScript reverse transcriptase®, Bio-Rad, CA). The target cDNA was amplified by real-time PCR (SsoAdvanced Universal SYBR® Green Supermix, Bio-Rad, CA). Hypoxanthine-guanine phosphoribosyltransferase (HPRT) was used the reference gene to normalize. The $2^{-\Delta\Delta CT}$ was used for the relative quantification analysis.

Cell proliferation assay

To determine the inhibition of cell proliferation, 5×10^3 cells per well of PANC-1, Mia PaCa-2 and BxPC-3 cells were seeded in 96-well plates at triplicates and grown in appropriate media for 24 h. P15 and irrelevant aptamer were added to cells at 1 μM and harvested them at 12 hrs, 24 hrs and 48 hrs. Inhibition of cell proliferation was measured by MTT assay (Promega, Madison, WI) at the indicated time intervals.

Results

Naïve whole SELEX

To find potential biomarkers for pancreatic cancer, untargeted SELEX, called blind

SELEX, was performed on naïve whole cells. To allow pancreatic cancer specificity, another type of cancer cells, Huh7 (hepatocarcinoma cells) was used as negative cells to remove non-specific binding of aptamers as described previously (30). To increase the nuclease resistance, 2′F pyrimidine modified RNAs was used to construct RNA aptamer library pool by PCR and *in vitro* transcription (IVT) (Fig. 1A). After 14 rounds of SELEX, a highly enriched aptamer, P15, was selected: GGGAGACAAGAATAAACGCTCAAAGTTGCGGCCCAACCGTTTAATTCAGA ATAGTGTGATGCCTTCGACAGGAGGCTCACAACAGGC. Minimum energy structural analyses of P15 were carried out using NUPACK software (http://www.nupack.org) (Fig. 1B). As depicted, the calculated secondary structure of P15 contains several stem-loop regions.

P15 aptamer shows pancreatic cancer specificity and internalizes into cells

To determine the binding on PANC-1 cells, P15 interactions with PANC-1 cells, aptamer binding was assessed by flow cytometry. The flow cytometry analyses of P15 confirmed enriched cell surface binding to PANC-1 cells, compared to the initial non-selected RNA library. PANC-1 cells treated with Cy3-labelled P15 aptamers demonstrated significantly higher levels of positively stained cells (Fig. 1C). The binding affinity (K_D) of P15 to PANC-1 cells was determined to be 16.05 nM (Fig. 1D). To verify the specificity of P15 to pancreatic cancer cells, a panel of four different pancreatic cancer cell lines (AsPC-1, CFPAC, MIA PaCa-2 and BxPC-3) was treated with Cy3-labelled P15 aptamer. Interestingly, punctate cytoplasmic staining was observed in pancreatic cancer cell lines, but no staining was observed in negative control cells (Huh7) (Fig. 2A). The pattern of cytoplasmic staining is suggestive of endocytic internalization

of aptamers. The internalization assay over time showed the increased the positive percentage and intensity on PANC-1 cells (Fig. 2B).

P15 aptamer binds to tumor associated cell surface vimentin

To identify the P15 binding ligand, cell membrane proteins were extracted and retrieved by biotinylated P15. The retrieved proteins were separated by SDS-PAGE followed by Coomassie staining to visualize the resolved protein bands (Fig. 3A). The highest matching peak retrieved from P15-treated cells matched a known peak for vimentin by LC-MS/MS spectrum (Fig. 3B right and left panel). To validate the LC-MS/MS results, a competition assay with vimentin antibodies was performed by live cell confocal and flow cytometry. Fluorescence intensity was measured by confocal microscopy. The antibodies to vimentin significantly reduced the binding of P15 to target cells, $P<0.05$ (Fig. 3C). Preincubation with anti-vimentin antibodies prevented the binding of P15 on PANC-1 by flow cytometry (Fig. 3D). These results strongly suggest the P15 bound to plasma membrane expressing vimentin on cancer cells. To confirm the direct binding of P15 with vimentin, surface plasmon resonance (SPR) with recombinant proteins and the colocalization assay on live cells were performed. In SPR assay, the increase in response units (RUs) from the baseline was measured and the calculated K_D by SPR was similar with the K_D determined with flow cytometry (Fig. 3E). In the colocalization assay, colocalization of Alexa 488-vimentin and Cy3-P15 were apparent in structures that appear yellow (Fig. 3F left) and overlayed spectrum in line profiling (Fig. 3F right). The overlap coefficient R value showed between 0.93 to 0.82, indicating the highly correlated colocalization of P15 and vimentin (Fig. 3F).

P15 aptamer inhibits the cell motility and invasiveness of pancreatic cancer cells

Vimentin is related with epithelial mesenchymal transition (EMT) during tumor metastasis (35). Since both cell migration and invasion have decisive role in the dissemination of cancer cells and metastasis, we further investigated the cell motility and invasion *in vitro*. For the motility of pancreatic cancer cells, a classic wound healing assay in which the cell monolayer was scratched and cells migrating to the wound area were monitored at different time points. Compared with control, the cells treated with P15 showed a wider wound distance after wound generation, and took a longer time to fill in the wound area, indicating a defect in migration (Fig. 4A and B).

Tumor migration assay was done using uncoated Boyden chamber to examine the *in vitro* invasion ability of tumor cells. Cells that migrated to the bottom of the transwells were directly quantified by visualization using phase-contrast. Compared with the control group, P15 treated groups (3000 nM and 1000 nM for 24, 36 and 48hrs incubation) displayed significantly inhibited cell migration (Fig. 4C). Groups treated with lower levels of P15 (333 nM and 111 nM) displayed cell invasiveness statistically equivalent to control (Fig. 4C). These results strongly indicate the P15 inhibits the tumor cell invasion. To figure out the nuclease resistance of P15, the serum stability of P15 in human and mice was assessed. Even though 2 F′ pyrimidine modified nucleotides was incorporated during the SELEX process to increase the nuclease resistance, the intensity of the band (representing the amount of intact aptamer) decreases with time, indicating degradation of the full-length of aptamer (Fig. 4D). The biological half-life of the P15 was about 3.37 hours in mice serum and 20.7 minutes in human serum (Fig. 4E).

P15 aptamer is associated with downregulation of MMP3

As vimentin is a biomarker for EMT, to investigate the downstream effects of P15 in EMT, EMT related gene expression was analyzed by PCR array after treatment of P15 in PANC-1. Among 84 key EMT related genes, five genes were identified as differently expressed genes (DEGs). In five DEGs, VCAN (Versican) and COL1A2 (Collagen, Type I, Alpha 2) were up-regulated. MMP3 (Matrix Metallopeptidase 3), IL1RN (Interleukin 1 Receptor Antagonist), and TWIST 1 (Twist Family BHLH Transcription Factor 1) were down-regulated compared with non-treated control (Fig. 5A). MMP3, an upregulated gene in EMT, was interestingly down-regulated in P15 treated cells in this study. To confirm the gene expression analysis by PCR array, relative quantitative real-time PCR was performed again. The consistent down-regulation of MMP3 showed in 24 hrs and 48 hrs after treatment of P15 (Fig. 5B).

To determine the effect of tumor cell proliferation by P15, MTT assay was performed as indicated time intervals. We observed that P15 did not inhibit the cell proliferation in MTT assay (Fig. 5C).

Discussion

Untargeted SELEX, also called “blind SELEX”, was employed to generate highly enriched RNA aptamers against pancreatic cancer cells. This strategy allows us to identify aptamers that bind specifically to PANC-1 cells. To identify aptamer binding ligands which might be used as potential biomarkers, the cell membrane was retrieved using affinity purification through the RNA aptamers. The aptamer-bound proteins were then identified by LC-MS/MS. Because LC-MS/MS does not require the samples be purified to a high degree of homogeneity (36) and works well as long as the target protein is a major component of the mixture (37), it the best choice in protein biomarker discovery. We have initiated this study to

discover new biomarkers for pancreatic cancer. Unexpectedly, the binding cell surface target of P15 was determined the cell surface vimentin on cancer cells by LC-MS/MS. The direct binding of P15 with vimentin was measured with SPR (Fig. 3E). The colocalization of P15 with vimentin was confirmed intracellularly (Fig. 3F), suggesting that the cell surface vimentin binding P15 aptamer is internalized into the pancreatic cancer cells.

Vimentin belongs to the group of intermediate filament proteins, which forms the cytoskeleton and associates with the nucleus, mitochondria, and ER (38). Vimentin, intracellular EMT tumor cell marker, is recently discovered as a mislocalized protein on the surface of metastatic cancer (39). The recruitment of vimentin to the cell surface is mediated by β3 integrin (16). Vimentin protein expression show 3-fold higher in pancreatic cancer than its expression in other type of cancers including lung, colon, and ovarian (40). It is reported that the presence of vimentin-expressing in pancreatic cancer predicts a shorter postsurgical survival (41). Vimentin expression is also correlated with epithelial mesenchymal transition (EMT) during tumor progression and metastasis (42). Targeting mislocalized cancer surface proteins is greatly improved the therapeutic interventions without harming normal cells. For the therapeutic use of P15, we hypothesized that P15 might be associated with the loss of invasion capabilities in tumor cells. Because the transition of cancer cells to invasive cell type via EMT is widely accepted as a pivotal role in tumor metastasis (35). To determine the therapeutic effects of P15, the tumor cell metastasis assay were performed *in vitro* platform. As suggested by our hypothesis, P15 showed the significant inhibition of tumor cell metastasis (Fig. 4A, B and C). However, P15 showed the lack of nuclease resistance in human and mice serum (Fig. 4D and E). As the aptamers can be reduced in size and be incorporated RNA analogues through chemical synthesis (43), to confer

the nuclease resistance of P15 for *in vivo* assays and clinical trials, the truncation of P15 with 2′-O-methyl modified nucleotides will be investigated in future studies.

For further investigation of the downstream effects of P15 on EMT, 84 key genes involved in EMT were profiled using the Human Epithelial to Mesenchymal Transition (EMT) RT² PCR Array. Among the five DEGs, interestingly, our data showed the down-regulated expression of MMP3 in P15 treated cells based on the results of gene expression analysis (Fig. 5A and B). Generally, MMP3 is an upregulated gene in EMT progression (44) and related to metastasis (45). For the biological functions, MMP3 modulates the tumor microenvironment and cancer cell invasion (44). It is also associated with poorer patient prognosis in pancreatic cancer (46). Our study suggest that P15 is associated with the downregulation of MMP3. In the MTT assay, P15 did not inhibit the tumor cell proliferation, which is consistent with the reported results that tumor-produced MMP3 does not affect in tumor growth (47).

In summary, this is the first study to show that anti-vimentin aptamers inhibited tumor cell invasion and the downregulation of MMP3 is associated with it. Moreover, the anti-vimentin aptamer P15, might be an effective anti-metastatic drug for use in the treatment of pancreatic cancer.

Disclosure of Potential Conflict of Interest: S.Y., N.H., and J.J.R. hold stocks in Apterna Ltd. U.K.

Author's Contributions: S.Y., J.R. and N.H. developed the concept, designed the experiments and prepared the manuscript. S.Y. performed RNA aptamer selection, cell internalization, measurements of cell binding affinity, ligand identification by MASS-SPEC, qPCR, SPR, data

organization, and statistical analyses. B.A. was involved in the chemotaxis assays, wound healing assays and co-localization assays.

Acknowledgements: We would like to thank the Shared Resources at the Beckman Research Institute of City of Hope for their technical assistance in analytical cytometry, light microscopy digital imaging, and mass spectrometry and proteomics core for technical assistance. Research reported in this publication included work performed in the analytical cytometry core supported by the National Cancer Institute of the National Institutes of Health under award number P30CA033572. The content is solely the responsibility of the authors and does not necessarily represent the official views of the National Institutes of Health. The authors wish to acknowledge funding from the National Institutes of Health R01 AI029329 and Apterna Ltd.

References

1. Ulrich H, Magdesian MH, Alves MJ, Colli W. In vitro selection of RNA aptamers that bind to cell adhesion receptors of Trypanosoma cruzi and inhibit cell invasion. J Biol Chem **2002**;277(23):20756-62.
2. Wang J, Jiang H, Liu F. In vitro selection of novel RNA ligands that bind human cytomegalovirus and block viral infection. RNA **2000**;6(4):571-83.
3. Blank M, Weinschenk T, Priemer M, Schluesener H. Systematic evolution of a DNA aptamer binding to rat brain tumor microvessels. selective targeting of endothelial regulatory protein pigpen. J Biol Chem **2001**;276(19):16464-8.
4. Daniels DA, Chen H, Hicke BJ, Swiderek KM, Gold L. A tenascin-C aptamer identified by tumor cell SELEX: systematic evolution of ligands by exponential enrichment. Proceedings of the National Academy of Sciences of the United States of America **2003**;100(26):15416-21.
5. Hicke BJ, Marion C, Chang YF, Gould T, Lynott CK, Parma D*, et al.* Tenascin-C aptamers are generated using tumor cells and purified protein. J Biol Chem **2001**;276(52):48644-54.
6. Wilson DS, Szostak JW. In vitro selection of functional nucleic acids. Annu Rev Biochem **1999**;68:611-47.
7. Ellington AD, Szostak JW. In vitro selection of RNA molecules that bind specific ligands. Nature **1990**;346(6287):818-22.
8. Tuerk C. Using the SELEX combinatorial chemistry process to find high affinity nucleic acid ligands to target molecules. Methods in molecular biology **1997**;67:219-30.
9. Berezovski MV, Lechmann M, Musheev MU, Mak TW, Krylov SN. Aptamer-facilitated biomarker discovery (AptaBiD). Journal of the American Chemical Society **2008**;130(28):9137-43.
10. Multhoff G, Botzler C, Wiesnet M, Muller E, Meier T, Wilmanns W*, et al.* A stress-inducible 72-kDa heat-shock protein (HSP72) is expressed on the surface of human tumor cells, but not on normal cells. International journal of cancer Journal international du cancer **1995**;61(2):272-9.
11. Ferrarini M, Heltai S, Zocchi MR, Rugarli C. Unusual expression and localization of heat-shock proteins in human tumor cells. International journal of cancer Journal international du cancer **1992**;51(4):613-9.
12. Ullrich SJ, Robinson EA, Law LW, Willingham M, Appella E. A mouse tumor-specific transplantation antigen is a heat shock-related protein. Proceedings of the National Academy of Sciences of the United States of America **1986**;83(10):3121-5.
13. Trepel J, Mollapour M, Giaccone G, Neckers L. Targeting the dynamic HSP90 complex in cancer. Nature reviews Cancer **2010**;10(8):537-49.
14. Li J, Lee AS. Stress induction of GRP78/BiP and its role in cancer. Current molecular medicine **2006**;6(1):45-54.
15. Lee AS, Hendershot LM. ER stress and cancer. Cancer biology & therapy **2006**;5(7):721-2.
16. Bhattacharya R, Gonzalez AM, Debiase PJ, Trejo HE, Goldman RD, Flitney FW*, et al.* Recruitment of vimentin to the cell surface by beta3 integrin and plectin mediates adhesion strength. Journal of cell science **2009**;122(Pt 9):1390-400.

17. Christian S, Pilch J, Akerman ME, Porkka K, Laakkonen P, Ruoslahti E. Nucleolin expressed at the cell surface is a marker of endothelial cells in angiogenic blood vessels. The Journal of cell biology **2003**;163(4):871-8.
18. Fogal V, Sugahara KN, Ruoslahti E, Christian S. Cell surface nucleolin antagonist causes endothelial cell apoptosis and normalization of tumor vasculature. Angiogenesis **2009**;12(1):91-100.
19. Panicot-Dubois L, Aubert M, Franceschi C, Mas E, Silvy F, Crotte C, *et al.* Monoclonal antibody 16D10 to the C-terminal domain of the feto-acinar pancreatic protein binds to membrane of human pancreatic tumoral SOJ-6 cells and inhibits the growth of tumor xenografts. Neoplasia **2004**;6(6):713-24.
20. Dua P, Kang HS, Hong SM, Tsao MS, Kim S, Lee DK. Alkaline phosphatase ALPPL-2 is a novel pancreatic carcinoma-associated protein. Cancer research **2013**;73(6):1934-45.
21. Yang M, Jiang G, Li W, Qiu K, Zhang M, Carter CM, *et al.* Developing aptamer probes for acute myelogenous leukemia detection and surface protein biomarker discovery. J Hematol Oncol **2014**;7:5.
22. Van Simaeys D, Turek D, Champanhac C, Vaizer J, Sefah K, Zhen J, *et al.* Identification of cell membrane protein stress-induced phosphoprotein 1 as a potential ovarian cancer biomarker using aptamers selected by cell systematic evolution of ligands by exponential enrichment. Analytical chemistry **2014**;86(9):4521-7.
23. Shangguan D, Cao Z, Meng L, Mallikaratchy P, Sefah K, Wang H, *et al.* Cell-specific aptamer probes for membrane protein elucidation in cancer cells. Journal of proteome research **2008**;7(5):2133-9.
24. Tanaka Y, Akagi K, Nakamura Y, Kozu T. RNA aptamers targeting the carboxyl terminus of KRAS oncoprotein generated by an improved SELEX with isothermal RNA amplification. Oligonucleotides **2007**;17(1):12-21.
25. Siegel RL, Miller KD, Jemal A. Cancer statistics, 2016. CA: a cancer journal for clinicians **2016**;66(1):7-30.
26. Malvezzi M, Bertuccio P, Levi F, La Vecchia C, Negri E. European cancer mortality predictions for the year 2013. Annals of oncology : official journal of the European Society for Medical Oncology **2013**;24(3):792-800.
27. Mayo SC, Nathan H, Cameron JL, Olino K, Edil BH, Herman JM, *et al.* Conditional survival in patients with pancreatic ductal adenocarcinoma resected with curative intent. Cancer **2012**;118(10):2674-81.
28. Kamisawa T, Isawa T, Koike M, Tsuruta K, Okamoto A. Hematogenous metastases of pancreatic ductal carcinoma. Pancreas **1995**;11(4):345-9.
29. Disibio G, French SW. Metastatic patterns of cancers: results from a large autopsy study. Archives of pathology & laboratory medicine **2008**;132(6):931-9.
30. Yoon S, Huang KW, Reebye V, Mintz P, Tien YW, Lai HS, *et al.* Targeted Delivery of C/EBPalpha -saRNA by Pancreatic Ductal Adenocarcinoma-specific RNA Aptamers Inhibits Tumor Growth In Vivo. Molecular therapy : the journal of the American Society of Gene Therapy **2016**;24(6):1106-16.
31. Sefah K, Shangguan D, Xiong X, O'Donoghue MB, Tan W. Development of DNA aptamers using Cell-SELEX. Nature protocols **2010**;5(6):1169-85.

32. Shevchenko A, Tomas H, Havlis J, Olsen JV, Mann M. In-gel digestion for mass spectrometric characterization of proteins and proteomes. Nature protocols **2006**;1(6):2856-60 doi 10.1038/nprot.2006.468.
33. Liang CC, Park AY, Guan JL. In vitro scratch assay: a convenient and inexpensive method for analysis of cell migration in vitro. Nature protocols **2007**;2(2):329-33.
34. Shaw LM. Tumor cell invasion assays. Methods in molecular biology **2005**;294:97-105.
35. Davis FM, Stewart TA, Thompson EW, Monteith GR. Targeting EMT in cancer: opportunities for pharmacological intervention. Trends in pharmacological sciences **2014**;35(9):479-88.
36. Hunt DF, Yates JR, 3rd, Shabanowitz J, Winston S, Hauer CR. Protein sequencing by tandem mass spectrometry. Proceedings of the National Academy of Sciences of the United States of America **1986**;83(17):6233-7.
37. Fitton JE, Dell A, Shaw WV. The amino acid sequence of the delta haemolysin of Staphylococcus aureus. FEBS letters **1980**;115(2):209-12.
38. Fuchs E, Weber K. Intermediate filaments: structure, dynamics, function, and disease. Annual review of biochemistry **1994**;63:345-82.
39. Mitra A, Satelli A, Xia X, Cutrera J, Mishra L, Li S. Cell-surface Vimentin: A mislocalized protein for isolating csVimentin(+) CD133(-) novel stem-like hepatocellular carcinoma cells expressing EMT markers. International journal of cancer **2015**;137(2):491-6.
40. Hong SH, Misek DE, Wang H, Puravs E, Hinderer R, Giordano TJ, *et al.* Identification of a Specific Vimentin Isoform That Induces an Antibody Response in Pancreatic Cancer. Biomarker insights **2006**;1:175-83.
41. Handra-Luca A, Hong SM, Walter K, Wolfgang C, Hruban R, Goggins M. Tumour epithelial vimentin expression and outcome of pancreatic ductal adenocarcinomas. British journal of cancer **2011**;104(8):1296-302.
42. Kokkinos MI, Wafai R, Wong MK, Newgreen DF, Thompson EW, Waltham M. Vimentin and epithelial-mesenchymal transition in human breast cancer--observations in vitro and in vivo. Cells, tissues, organs **2007**;185(1-3):191-203.
43. Que-Gewirth NS, Sullenger BA. Gene therapy progress and prospects: RNA aptamers. Gene Ther **2007**;14(4):283-91.
44. Radisky ES, Radisky DC. Matrix metalloproteinase-induced epithelial-mesenchymal transition in breast cancer. Journal of mammary gland biology and neoplasia **2010**;15(2):201-12.
45. Mendes O, Kim HT, Stoica G. Expression of MMP2, MMP9 and MMP3 in breast cancer brain metastasis in a rat model. Clinical & experimental metastasis **2005**;22(3):237-46.
46. Mehner C, Miller E, Nassar A, Bamlet WR, Radisky ES, Radisky DC. Tumor cell expression of MMP3 as a prognostic factor for poor survival in pancreatic, pulmonary, and mammary carcinoma. Genes & cancer **2015**;6(11-12):480-9.
47. McCawley LJ, Wright J, LaFleur BJ, Crawford HC, Matrisian LM. Keratinocyte expression of MMP3 enhances differentiation and prevents tumor establishment. The American journal of pathology **2008**;173(5):1528-39.

FIGURE LEGENDS

Figure 1. Naïve cell SELEX and Binding affinity. **A**, Schematic untargeted live-cell SELEX procedures. The DNA library contained 40 nt of random sequences was synthesized and amplified by PCR. 2′F modified RNA aptamer library was synthesized throughout in vitro transcription. To remove non-specific binding, aptamer library pools were incubated on Huh7 cells as the negative cells. The supernatant was again incubated on PANC-1 cells for positive selection. Total RNA was extracted and amplified through polymerase chain reaction (PCR) and in vitro transcription (IVT). The RNA aptamer selection was repeated for 14 rounds of SELEX. **B**, P15 was selected from a randomized N40 RNA library, after 14 rounds of SELEX. The secondary structure of P15 was predicted using NUPACK software. **C,** Cy3-labeled P15 aptamers (200 nM) were assessed for binding efficiency by flow cytometry in PANC-1 and control Huh7 cells. Data show from triplicate experiments. Huh7 CC (Huh7 unstained cell control), PANC-1 CC (PANC-1 unstained cell control), Huh7 Lib (Huh 7 staining control with a Cy3-labeled library), PANC-1 Lib (PANC-1 staining control with a Cy3-labeled library), Huh7 P15 (Huh7 stained with P15), PANC-1 P15 (PANC-1 stained with P15). **D**, The dissociation constant (K_D) was measured by flow cytometry using increasing concentrations of Cy3-labeled aptamers (15.6 to 500 nM). Mean fluorescence intensity (MFI) was measured and calculated using a one-site binding model for non-linear regression.

Figure 2. Internalization of P15**. A**, Cell internalization was assessed on live cells. The pancreatic cell lines PANC-1, AsPC-1, CFPAC-1, MIA PaCa-2, BxPC-3 and Huh7 were treated

with 100 nM of final concentration of the Cy3-labeled P15 aptamer and analyzed by confocal microscopy. All pancreatic lines show punctate regions of Cy3 labeling. The Huh7 negative cells showed negative staining. Red: Cy3-labeled RNA. Blue: Hoechst 33342. Scale bar: 10 μm. **B**, Quantitative internalization assay over time in live cells. The PANC-1 were treated with 200 nM of final concentration of the Cy3-labeled P15 aptamer and incubated for the indicated time interval. The percentage of internalization was assessed by confocal microscopy in different locations at each time points (N=7-11).

Figure 3. Tandem MS/MS spectra of aptamer binding ligand. **A**, Polyacrylamide gel electrophoresis (SDS-PAGE) was used to separate immobilized protein samples after pulldown with biotinylated P15 and negative control RNAs. Coomassie-stained gels M (Marker), total cell lysate (lane 1), P15 (lane 2), NC (irrelevant RNA, lane 3). Arrow indicates target. **B**, Peptide matching and MS/MS spectrum of P15 affinity-purified peptides. Inset: Amino acid sequence of the parent peptide showing b- and y-ion series coverage. Target epitopes are highlighted in yellow. **C**, An aptamer-antibody competition assay was used to validate the target. Cy3-labeled P15 aptamer was used to compete with vimentin antibodies in PANC-1. P15-VIM-NC; P15 treated without vimentin antibodies. P15-VIM-competition; P15 treated with vimentin antibodies. Bound P15 was calculated using fluorescence intensity (AU: arbitrary units). Student's t test was used for the statistical significance analysis. (N=10) *: $P \leq 0.05$. **D**, Flow cytometry based competition assay. After preincubation with vimentin antibodies, Cy3-labeled aptamers at 200 nM of final concentration were added and incubated with 2×10^5 cells for 30 minutes on ice. Reduction of binding was observed in vimentin antibody treated group. P15-VIM-NC; P15 treated without vimentin antibodies. P15-VIM-competition; P15 treated with vimentin antibodies.

E. The SPR sensorgrams of binding P15 with vimentin. For the binding assay of P15 aptamer–vimentin by SPR, the Biacore T100 was used to monitor label-free interaction of P15 with vimentin. The increase in response units (RUs) from the baseline was measured. BIAevaluation software was used to measure the binding affinity. **F**, The Colocalization of P15 with vimentin on live cells. After co-incubation of P15 with anti-vimentin antibodies for 1 hour at 37 °C in PANC-1, colocalization of P15 with vimentin was analyzed with Zeiss LSM scanning microscopy with Airyscan. The correlation R value of Alexa 488 and Cy3 appearing yellow was indicated on left top corner in three different positions. Red: Cy3 labeled P15, Green: Anti-vimentin with Alexa 488. Blue: Hoechst 33342. Scale bar: 5 μm. The colocalization of Alexa 488-vimentin and Cy3-P15 appeared yellow (left) and overlayed spectrum in line profiling (right).

Figure 4. Cell migration and invasion assays. **A**, Phase contrast images of wound healing assay were taken at 0 h (immediately after scratching) and at the indicated time intervals in irrelevant aptamer (top panels) and the wound open in P15 treated cells (down panels). 3 μM of final concentration of folded P15 was added into media after scratching. Control (irrelevant aptamers) showed the wound closure at 20 hours. Scale bar = 100 μm. **B**, The results of wound healing assay represented the mean of three measures of each wounded area. Error bars indicate mean ± standard deviation (N=3). Student's t test was used for the statistical significance analysis. *: $P \leq 0.05$. **: $P \leq 0.01$, ***: $P \leq 0.001$. **C**, Chemotaxis cell invasion assay by IncuCyte live-cell imaging system. Integrated metrics quantified the chemotactic response using 1,000 cells per well. Data was normalized to negative control. Each group is shown in quadruplicate. Student's t test was used for the statistical significance analysis. *: $P \leq 0.05$. **: $P \leq 0.01$, ***: $P \leq 0.001$. **D**,

Serum stability of P15 in human and mice serum. Folded P15 was incubated in 50 % of human and mice serum for indicated time intervals at 37 °C and the aptamer samples were separated by denaturing PAGE gel electrophoresis. **E**, The intact aptamer (%) was plotted as a function of the incubation time (0 to 48 hours) and fitted using a non-linear one-phase decay model (GraphPad).

Figure 5. EMT-related gene profiling and cell proliferation assay. **A**, 84 key genes involved in EMT were profiled by the Human Epithelial to Mesenchymal Transition (EMT) RT² Profiler PCR Array. VCAN and COL1A2 were up-regulated. MMP3, IL1RN and TWIST 1 were down-regulated in P15 treated PANC-1. **B**, Relative transcript expression for MMP3 mRNA was quantified by real-time PCR. HPRT was used for the housekeeping gene to normalize. One way ANOVA test was used for the statistical significance analysis. *: $P \leq 0.05$. **: $P \leq 0.01$, ***: $P \leq 0.001$. **C**, Cell proliferation assay was performed by MTT assay. No significant results have been observed. One way ANOVA test was used for the statistical significance analysis.

Figure.1

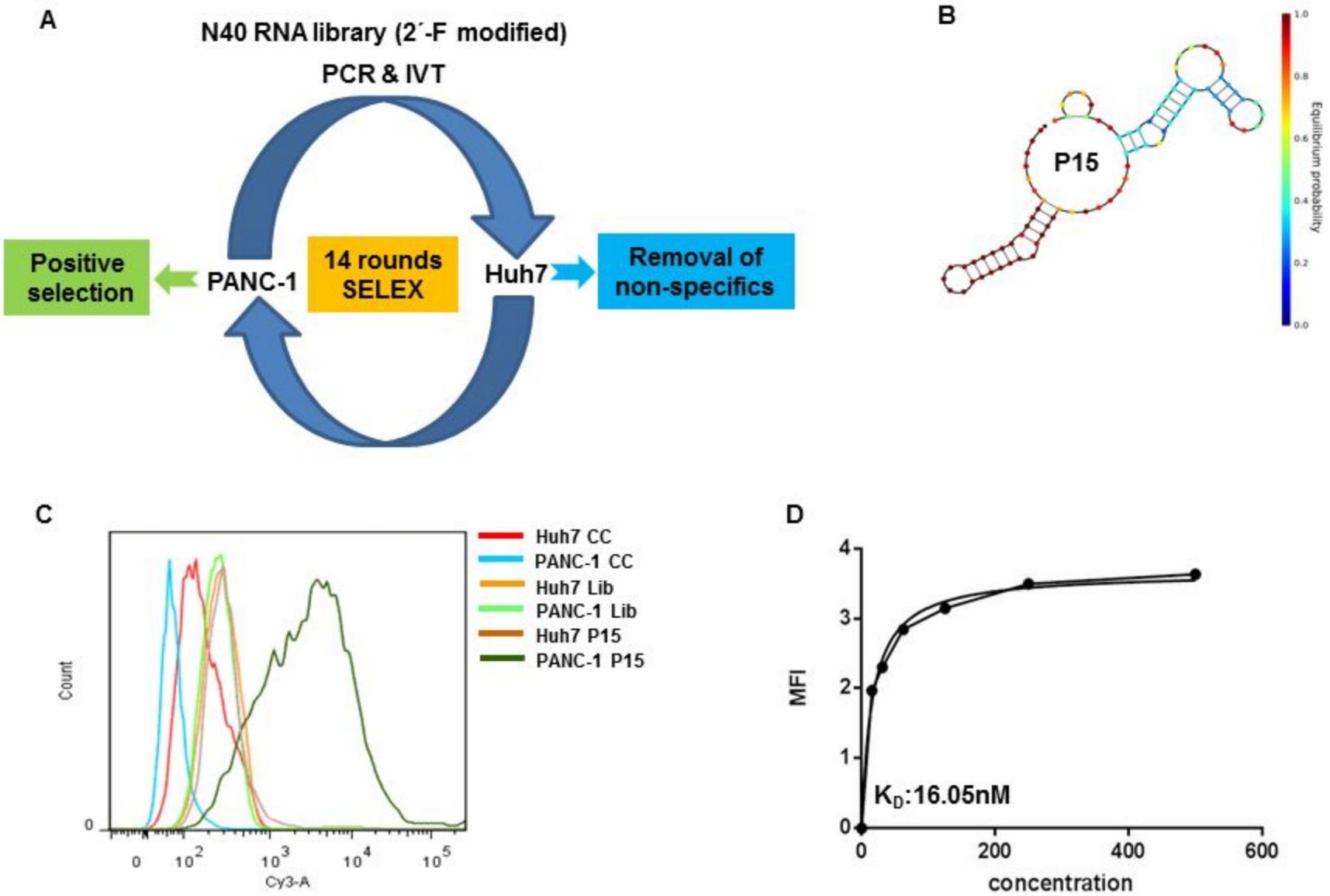

Figure.2

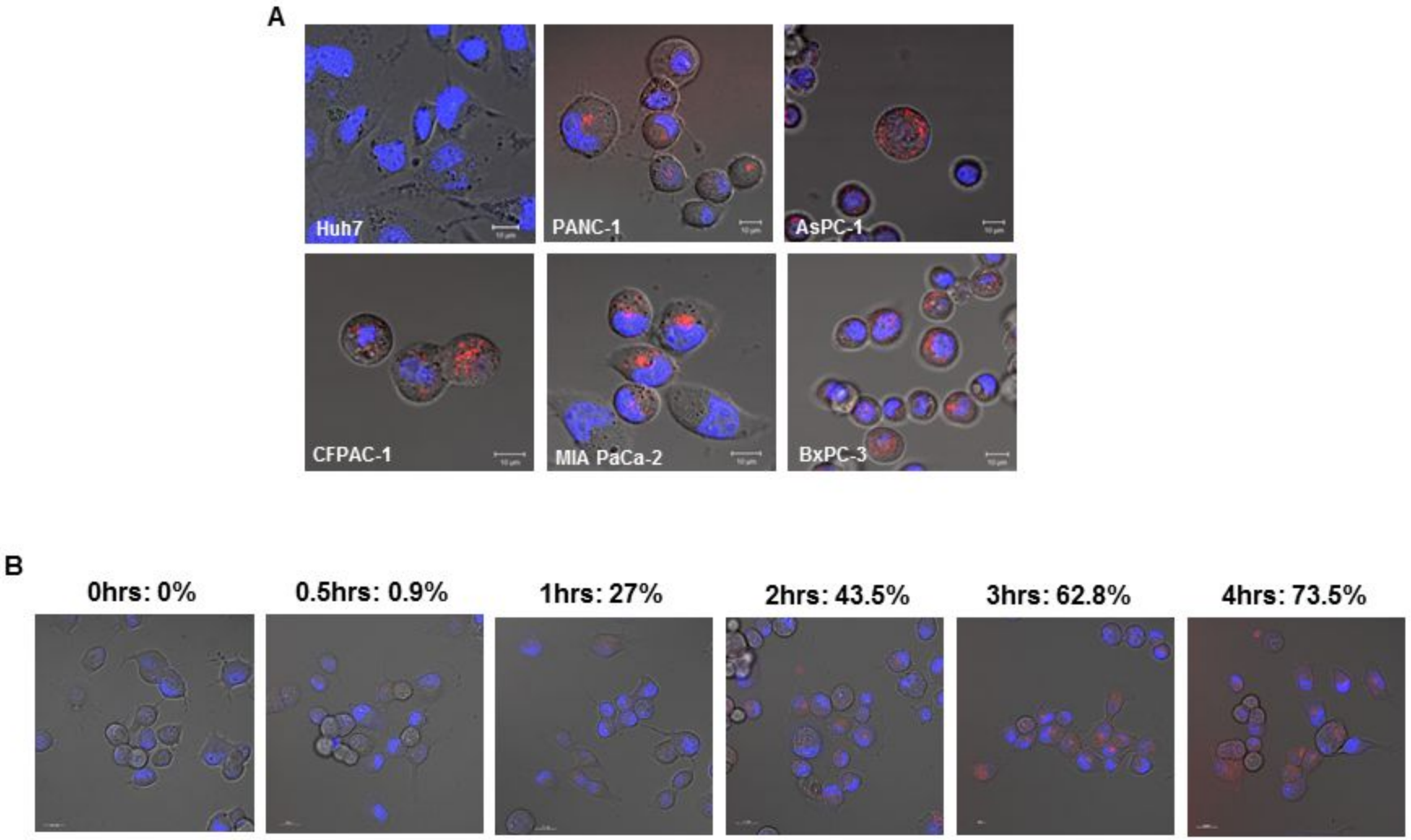

Figure.3

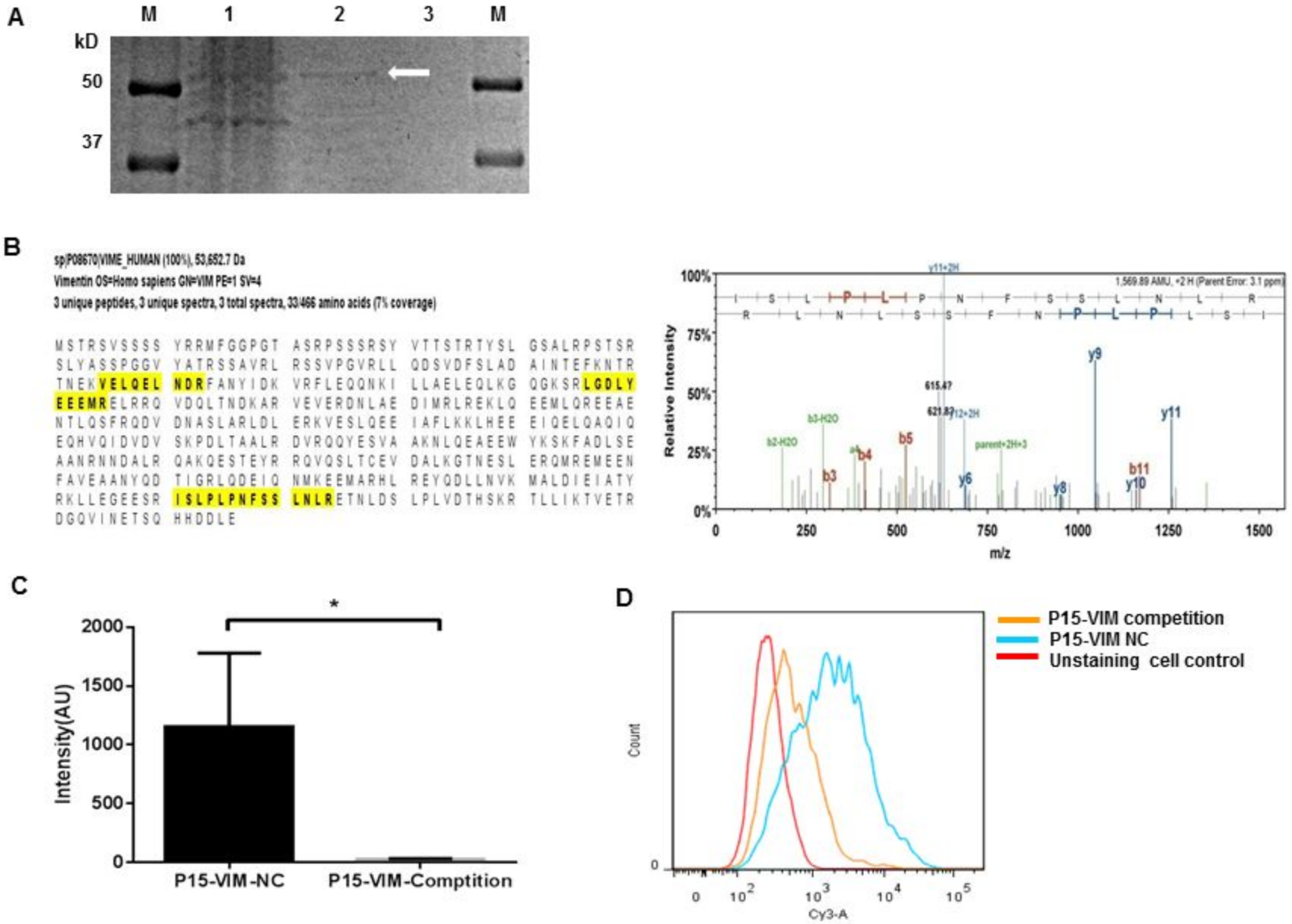

E

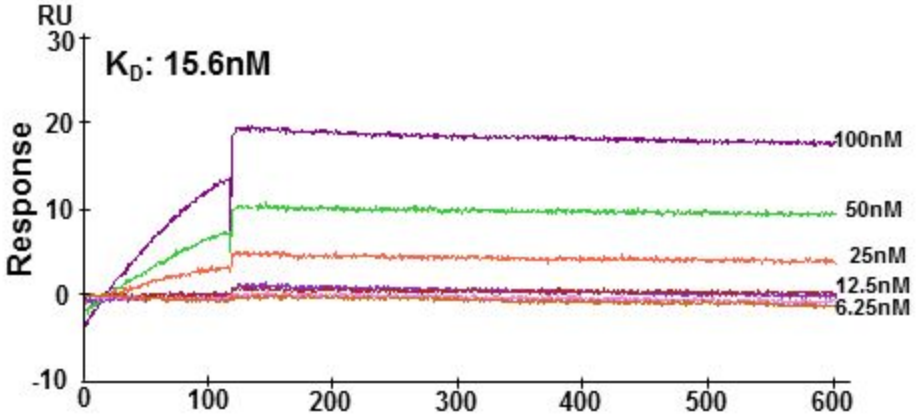

F

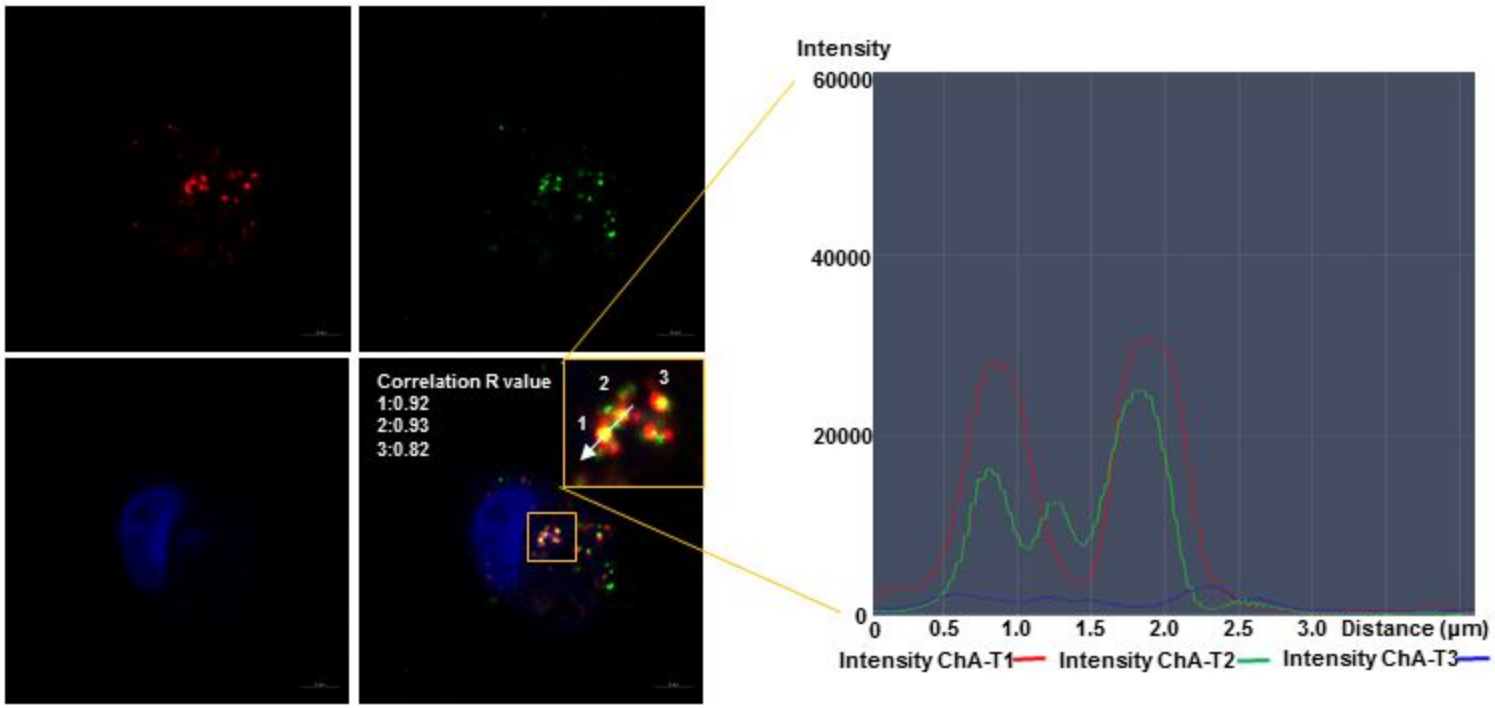

Figure.4

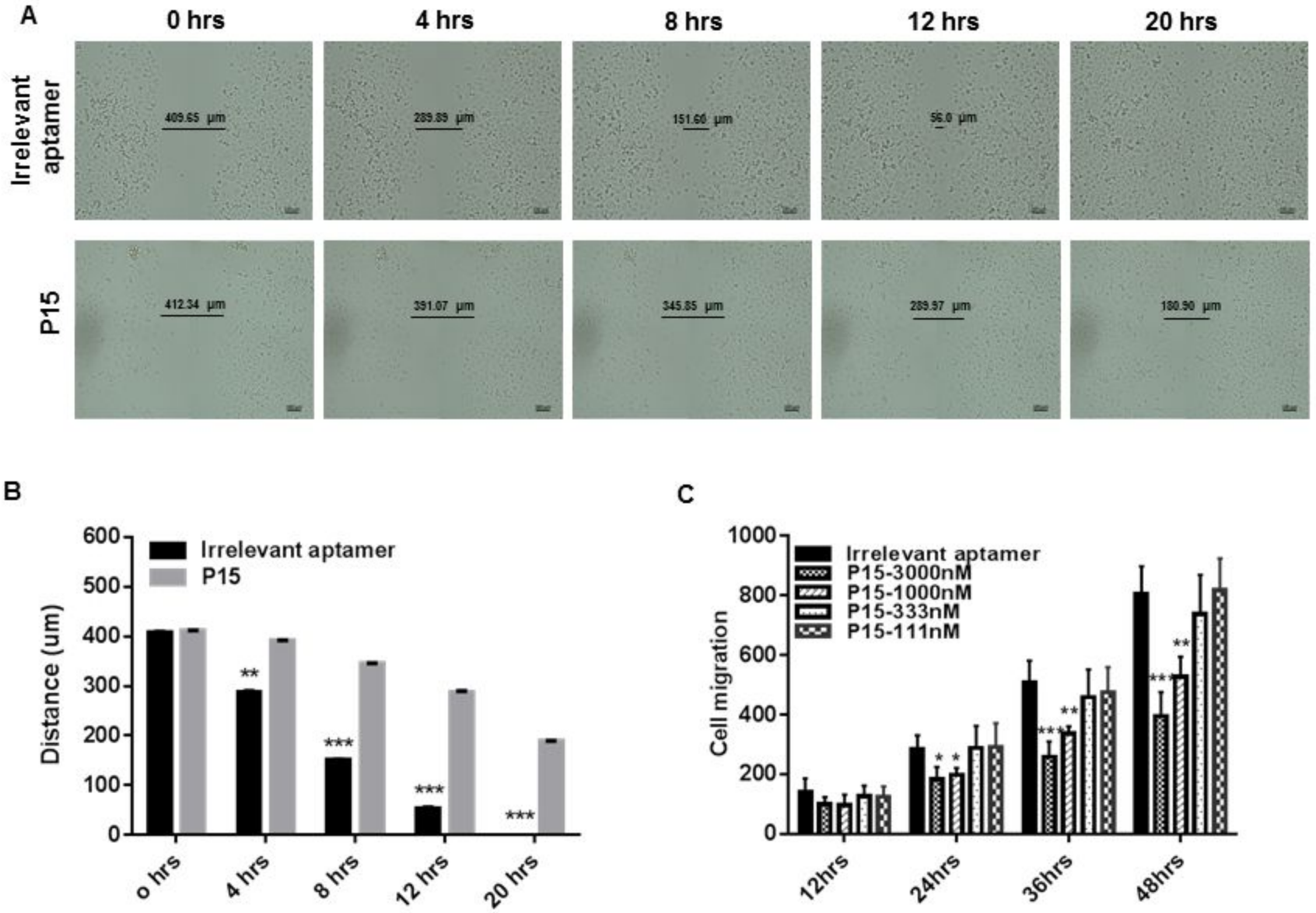

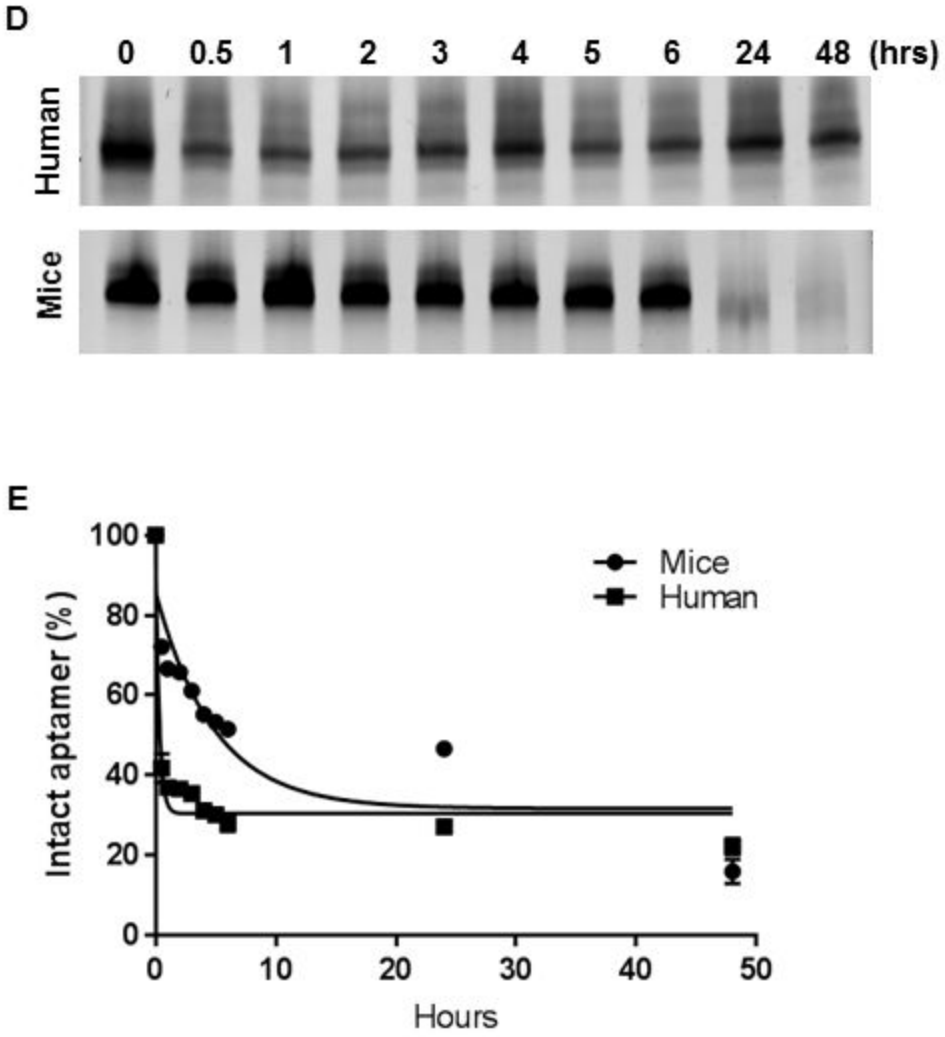

Figure.5

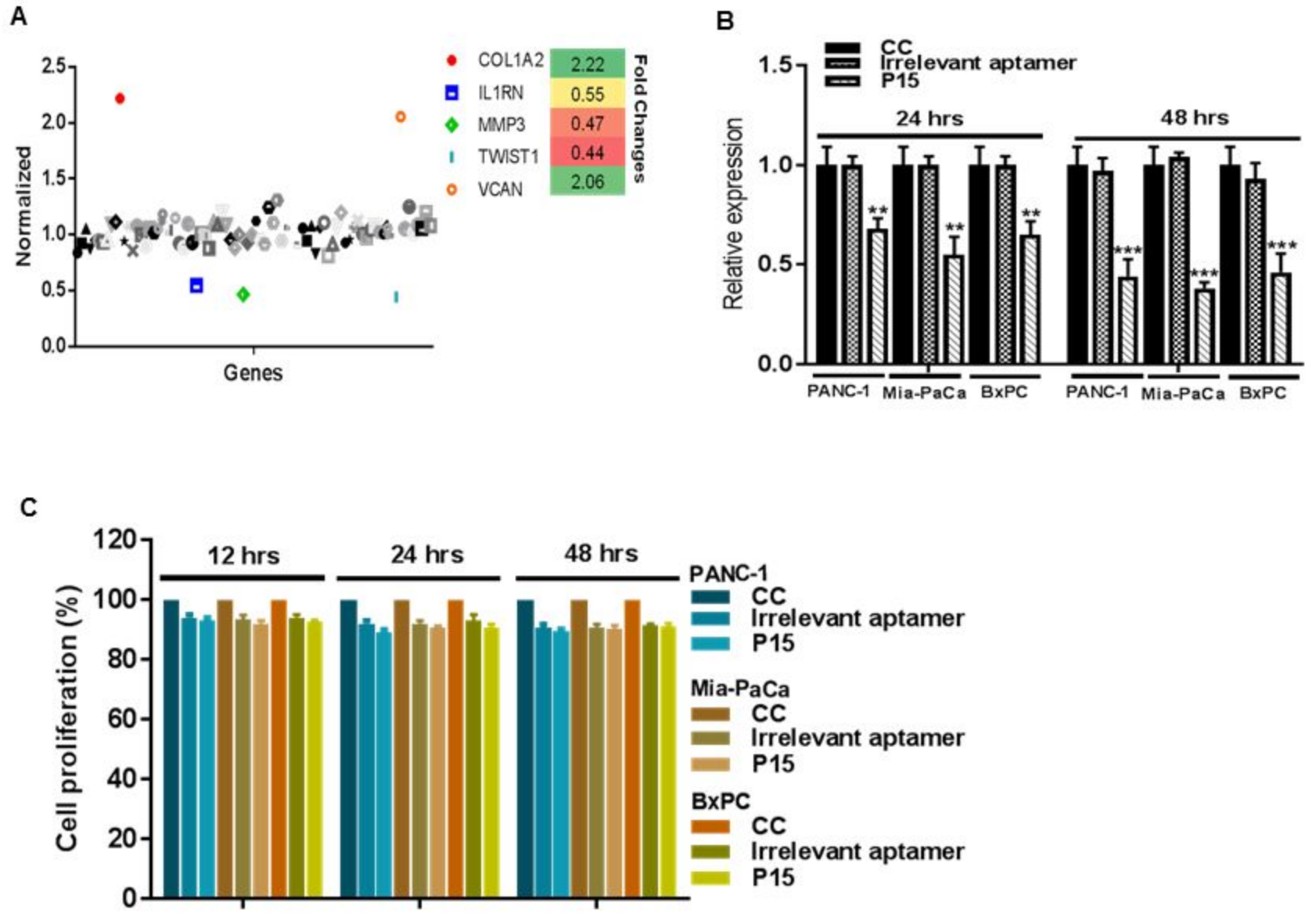

AACR American Association for Cancer Research

Molecular Cancer Research

Blind SELEX Approach Identifies RNA Aptamer that Regulate EMT and Inhibit Metastasis

Sorah Yoon, Brian Armstrong, Nagy Habib, et al.

Mol Cancer Res Published OnlineFirst April 10, 2017.